THE JOURNAL OF PHYSICAL CHEMISTRY B

Article

pubs.acs.org/JPCB

Kinetic and Thermodynamic Origins of Osmolyte-Influenced Nucleic Acid Folding

Erik D. Holmstrom, Nicholas F. Dupuis, and David J. Nesbitt*

JILA, University of Colorado and National Institute of Standards and Technology, and Department of Chemistry and Biochemistry, University of Colorado, Boulder, Colorado 80309-0440, United States

Supporting Information

ABSTRACT: The influential role of monovalent and divalent metal cations in facilitating conformational transitions in both RNA and DNA has been a target of intense biophysical research efforts. However, organic neutrally charged cosolutes can also significantly alter nucleic acid conformational transitions. For example, highly soluble small molecules such as trimethylamine N-oxide (TMAO) and urea are occasionally utilized by organisms to regulate cellular osmotic pressure. Ensemble studies have revealed that these so-called osmolytes can substantially influence the thermodynamics of nucleic acid conformational transitions. In the present work, we exploit single-molecule FRET (smFRET) techniques to measure, for first time, the kinetic origins of these osmolyte-induced changes to the folding free energy. In particular, we focus on smFRET RNA and DNA constructs designed as model systems for secondary and tertiary structure formation. These findings reveal that TMAO preferentially stabilizes both secondary and tertiary interactions by increasing k_{fold} and decreasing k_{unfold}, whereas urea destabilizes both conformational transitions, resulting in the exact opposite shift in kinetic rate constants (i.e., decreasing k_{fold} and increasing k_{unfold}). Complementary temperature-dependent smFRET experiments highlight a thermodynamic distinction between the two different mechanisms responsible for TMAO-facilitated conformational transitions, while only a single mechanism is seen for the destabilizing osmolyte urea. Finally, these results are interpreted in the context of preferential interactions between osmolytes, and the solvent accessible surface area (SASA) associated with the (i) nucleobase, (ii) sugar, and (iii) phosphate groups of nucleic acids in order to map out structural changes that occur during the conformational transitions.

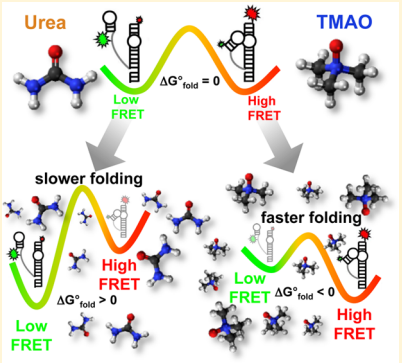

1. INTRODUCTION

Nucleic acid folding free energies are significantly influenced by the presence of various aqueous cosolutes. Metal cations obviously represent some of the most prominent and well-studied cosolutes and are known to be important for a large number of nucleic acid conformational transitions ranging in complexity from short, single-strand oligonucleotides[1] to large, highly organized RNAs like the large ribosomal subunit.[2] However, metal ions are certainly not the only cosolutes that can alter the energetics of nucleic acid folding. Indeed, as the primary focus of this work, we investigate the influence of osmolytes, which are highly soluble small organic molecules utilized by organisms to regulate osmotic pressure. Of particular relevance, these biologically relevant, nonmetallic cosolutes have also been shown to affect the stability of many nucleic acid structural motifs.[3−5]

Early work on the biological importance of osmolytes has demonstrated that they help living cells respond to changes in osmotic pressure.[6,7] More interestingly, however, numerous experiments have shown that high concentrations of osmolytes can either promote or inhibit folding of nucleic acids[4] and proteins,[8] depending on the chemical nature of the osmolyte. As intracellular concentrations change in response to osmotic stress, the effects of these cosolutes on the energetics of structured proteins and nucleic acids must therefore be counterbalanced in order to maintain homeostasis. Previous biological studies have validated this idea by demonstrating that some organisms are able to adjust intracellular concentrations of stabilizing osmolytes to offset the effect of urea.[9,10]

Because osmolytes are known to alter the stability of biomolecules, a large number of scientific investigations have centered on studying their ability to influence protein[11−14] and nucleic acid[4,15−19] conformational transitions. Urea is one of the better known osmolytes and tends to destabilize folded proteins[20−22] and nucleic acids,[23−25] whereas trimethylamine *N*-oxide (TMAO) is a lesser known osmolyte that frequently stabilizes such biomolecular folding events.[15,24,26,27] Until recently, most research efforts were directed at understanding the interactions between osmolytes and proteins rather than nucleic acids.[3] We build on this growing interest by reporting the first, to our knowledge, detailed kinetic studies of osmolyte-influenced nucleic acid conformational transitions using single-molecule fluorescence techniques.

Received: December 15, 2014
Revised: January 22, 2015
Published: January 26, 2015

DOI: 10.1021/jp512491n
J. Phys. Chem. B 2015, 119, 3687−3696

Over the years, a number of experimental and theoretical efforts regarding TMAO[15,28,29] and urea[16,30−32] have brought about a more physical understanding of such nucleic acid-osmolyte interactions. Inspired by quantitative thermodynamic work on proteins,[14] recent ensemble studies indicate that osmolytes can interact with each of the (i) nucleobase, (ii) sugar, and (iii) phosphate components of a nucleic acid.[4,15,16] Specifically, these measurements demonstrated conclusively that urea destabilizes RNA folding transitions by forming favorable interactions with all three constituents, which increase in strength from urea-phosphate to urea-nucleobase.[16] Because unfolded conformations of most nucleic acids tend to have more solvent accessible surface area (SASA), urea will therefore preferentially stabilize such conformations relative to those that are folded and therefore more compact (Figure 1). This results in a net increase in free energy change for folding (ΔG°_{fold}), driven by folding-induced burial of nucleobase SASA. For this simple reason, urea is commonly thought of as a destabilizing osmolyte, as it promotes the unfolding process (Figure 1).

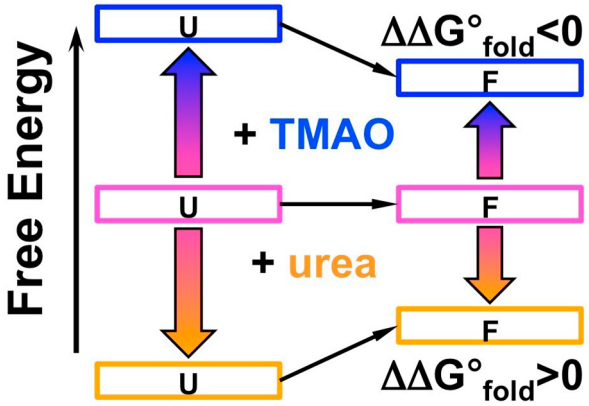

Figure 1. Free-energy diagram representing the effect of TMAO or urea on the stability of the unfolded (U) or folded (F) structures of a nucleic acid. TMAO has a more unfavorable interaction with the unfolded, rather than folded, structure, which results in a net decrease in ΔG°_{fold}. By way of contrast, urea has a more favorable interaction with the unfolded conformation, which gives rise to a net increase in ΔG°_{fold}.

Conversely, the presence of TMAO gives rise to the opposite effect, specifically a net decrease in ΔG°_{fold}. Such effects result primarily from unfavorable interactions between the osmolyte and the three nucleic acid components, which range from relatively strong TMAO-phosphate interactions to the rather weak TMAO-sugar interactions.[15] As described above, nucleic acids tend to become more compact when they fold, often resulting in burial of the phosphate SASA. Therefore, TMAO facilitates folding by virtue of preferential destabilization of the unfolded nucleic acid species, which results in a net stabilization of the folded conformation. Accordingly, TMAO is best-characterized as a stabilizing osmolyte (Figure 1).

To date, experimental studies investigating the influence of osmolytes on structured nucleic acid have been largely based on ensemble techniques (e.g., calorimetry or UV-spectroscopy), which only provide information about the equilibrium constant between folded and unfolded species (e.g., K_{eq} = [folded]/[unfolded]). Although such studies have been extremely informative, they have not been able to partition equilibrium effects into components related to the folding/unfolding kinetics (e.g., $K_{eq} = k_{fold}/k_{unfold}$). As a result, the kinetic origin of osmolyte-influenced nucleic acid folding remains poorly understood and represents a major focus of the present study.

Single-molecule fluorescence resonance energy transfer (smFRET) methods[33] are ideally suited to address such kinetic questions by providing information on the folding/unfolding rate constants under equilibrium conditions for a given nucleic acid conformational transition. Specifically, we have designed two fluorescently labeled constructs (Figure 2) as models systems for (i) secondary (e.g., DNA duplex association/dissociation) and (ii) tertiary (e.g., RNA loop docking/undocking) structure formation. The first is a well-characterized 8 bp DNA duplex,[34] which we use to elucidate the role of osmolytes in the formation of nucleic acid 2° structures (Figure 2, panels a and b). The second is an RNA construct that isolates the GAAA tetraloop—tetraloop receptor (TL-TLR) interaction from the *Tetrahymena* ribozyme.

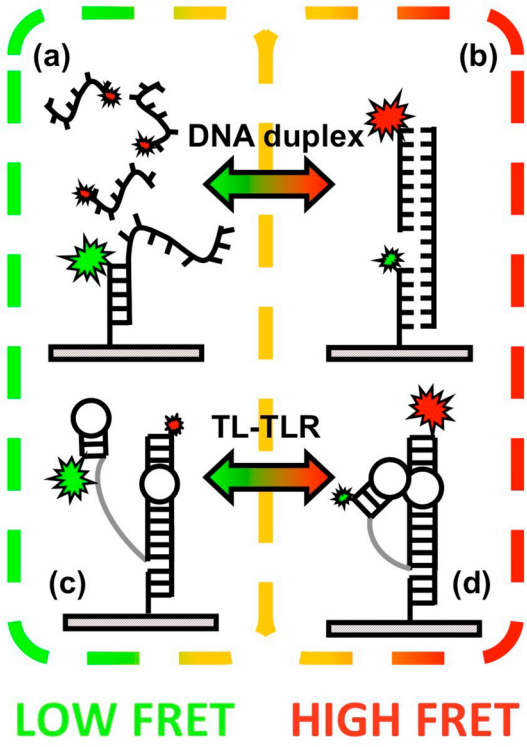

Figure 2. Cartoon representation of the two smFRET nucleic acid constructs used throughout this study. The DNA duplex construct (a and b) is intended to be a model system for the nucleic acid secondary structure, whereas the TL-TLR construct (c and d) serves as a model for RNA tertiary interactions. For both constructs, formation of the interaction (b and d), referred to as folding, results in an increase in E_{FRET} (a and c).

This ubiquitous loop−bulge interaction[35] has undergone extensive biophysical characterization at the single-molecule level[36−42] and is used as a model system to explore the influence of osmolytes on RNA tertiary structure formation (Figure 2, panels b and c). Utilizing smFRET techniques to study these model systems, we show that the kinetic origin of TMAO-facilitated nucleic acid folding arises from an increase in k_{fold} and a corresponding decrease in k_{unfold} for both 2° and 3° structure formation. Interestingly, however, quite the opposite is true for the kinetic origin of urea-inhibited nucleic acid structure formation, which is found to result from a decrease in k_{fold} and an increase in k_{unfold} for both types of conformational transitions.

DOI: 10.1021/jp512491n
J. Phys. Chem. B 2015, 119, 3687−3696

2. EXPERIMENTAL METHODS

2.1. Nucleic Acids. The smFRET DNA duplex construct consists of three custom oligonucleotides (Figure 2, panels a and b) as described previously[34] and therefore needs only a brief explanation. Strand 1 (5′- biotin-$(CA)_8$-Cy3-3′) has a biotin moiety for surface immobilization and a donor fluorophore for fluorescence resonance energy transfer (FRET). This is annealed to strand 2 (5′-TGGTTGGGGTT-$(TG)_8$-3′) to form a 16 bp dsDNA scaffold with a 11 nt 5′ overhang. Strand 3 (5′-CCCAACCAA-Cy5-3′), which contains a 3′ acceptor dye, can hybridize with the 8 of the 11 nt in the 5′ overhang, where the underlined nucleotides in strands 2 and 3 correspond to the 8bp DNA duplex examined in this work (Figure 2b). Throughout such a hybridization event, the Cy5 fluorophore of strand 3 remains in close proximity to the Cy3 fluorophore, allowing for efficient transfer of energy ($E_{FRET} \approx 0.7$) from the donor to the acceptor. However, upon dissociation of strand 3 from the 11 nt 5′ overhang, diffusion rapidly increases the distance between the donor and acceptor fluorophores (Figure 2a), thereby preventing energy transfer to the acceptor ($E_{FRET} \approx 0$). This yields two possible FRET states associated with the secondary structural transition of the 8bp DNA duplex construct: (i) associated (Figure 2b, high E_{FRET}) and (ii) dissociated (Figure 2a, low E_{FRET}).

The GAAA tetraloop—tetraloop receptor (TL-TLR) model system is a modified version[43] of a previously designed construct,[41] whereby a synthetic polyethylene glycol hexamer (PEG_6) linker is used to localize the GAAA tetraloop near its cognate receptor. For design flexibility, this construct is also built from three custom oligonucleotides (Figure 2, panels c and d). The Cy3-labeled RNA containing the GAAA tetraloop, as depicted in bold font (5′-Cy3-GGCGAAAGCC-PEG_6-CGUGUCGUCCUAAGUCGGC-3′), is annealed to a Cy5 labeled RNA (5′-Cy5-GCCGAUAUGGACGACACGCCCCUCAGACGAGUGCG-3′) to form the 11 nt receptor domain, indicated by the underlined nucleotides. This results in a 17 nt 3′ overhang that can hybridize to a 14 nt complementary DNA containing a 5′ biotin (5′-biotin-CGCACTCGTCTGAG-3′) for surface immobilization. Once completely annealed, this three-piece RNA construct serves as a FRET-labeled, biotinylated TL-TLR construct. Formation of this tertiary interaction reduces the distance between the donor and acceptor fluorophores, which increases the energy transfer efficiency from $E_{FRET} \approx 0.3$ to $E_{FRET} \approx 0.7$. This yields two distinct conformations for the TL-TLR RNA: (i) docked (Figure 2d, high E_{FRET}) and (ii) undocked (Figure 2c, low E_{FRET}).

2.2. Solution and Sample Preparation. Surface immobilization is accomplished via biotin−streptavidin chemistry. To attach the nucleic acids to a glass coverslip, the sample holder (10 μL) is consecutively flushed with 200 μL of the following three solutions: (i) 10 mg/mL bovine serum albumin (BSA) containing 10% biotinylated-BSA, (ii) 200 μg/mL streptavidin, and (iii) 100 pM biotinylated fluorescent-labeled nucleic acid. This procedure provides reproducible immobilization with surface densities of approximately 1 molecule per μm^2. Immediately prior to imaging with the fluorescence microscope, the sample holder is flushed with 200 μL of an imaging buffer (50 mM hemisodium HEPES, 5.0 mM PCA, 10 mM KOH, 100 nM PCD, 2.0 mM Trolox, 0.1 mM EDTA at pH ≈ 7.5) containing the desired concentrations of osmolytes (0−2 M) and KCl (either 50 or 100 mM KCl for experiments with the TL-TLR and 8 bp DNA duplex, respectively). The enzymatic oxygen scavenging system of PCD and PCA[44] is used to enhance the photostability of the cyanine dyes. For experiments involving the 8 bp DNA duplex, the imaging buffer also contains 200 nM freely diffusing Cy5 oligonucleotide, which permits observation of the corresponding bimolecular process at the single molecule level.

2.3. smFRET Microscope. All smFRET experiments are performed on an inverted confocal fluorescence microscope with a N.A. = 1.2 water objective (Figure 3). A 20 MHz repetition rate, 532 nm horizontally polarized laser beam overfills the limiting aperture of the optical system resulting in a diffraction-limited laser spot at the focus of the objective, which is used to directly excite the donor fluorophores of surface-immobilized RNA constructs. Fluorescent photons are collected in a standard epifluorescence optical configuration before being separated by color (i.e., donor vs acceptor) and polarization (i.e., horizontal vs vertical) and directed onto four single photon avalanche photo diodes (APDs), with a time-correlated single-photon counting (TCSPC) module recording the arrival of each photon. This information is used to construct time-traces of the donor (I_D) and acceptor (I_A) fluorescence intensity (Figure 4), which can readily be converted to FRET trajectories with eq 1, where α and Q correct for complications associated with direct excitation, cross talk, quantum yield, and collection efficiency (see ref 39 for further information).

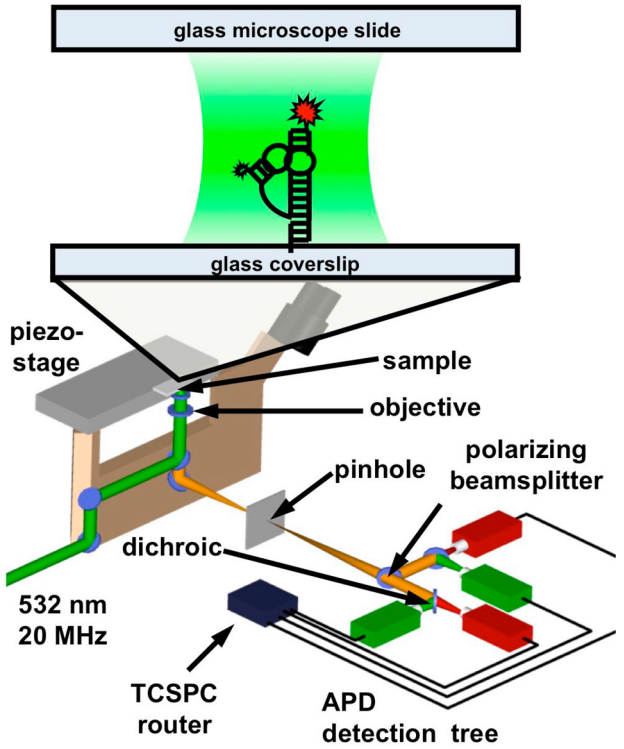

Figure 3. Schematic representation of the inverted confocal fluorescence microscope used to acquire smFRET trajectories. Individual molecules are immobilized to the glass coverslip using standard biotin−streptavidin chemistry (see Experimental Methods for details). Excitation and emission is achieved using standard epifluorescence techniques. Fluorescent photons are focused through a confocal pinhole before being separated by color and polarization and directed onto four single-photon avalanche photodiodes. Upon detection, the arrival times of individual photons are recorded and sent to a time-correlated single-photon counting (TCSPC) router where they are used to generate time trajectories of donor and acceptor fluorescence.

DOI: 10.1021/jp512491n
J. Phys. Chem. B 2015, 119, 3687−3696

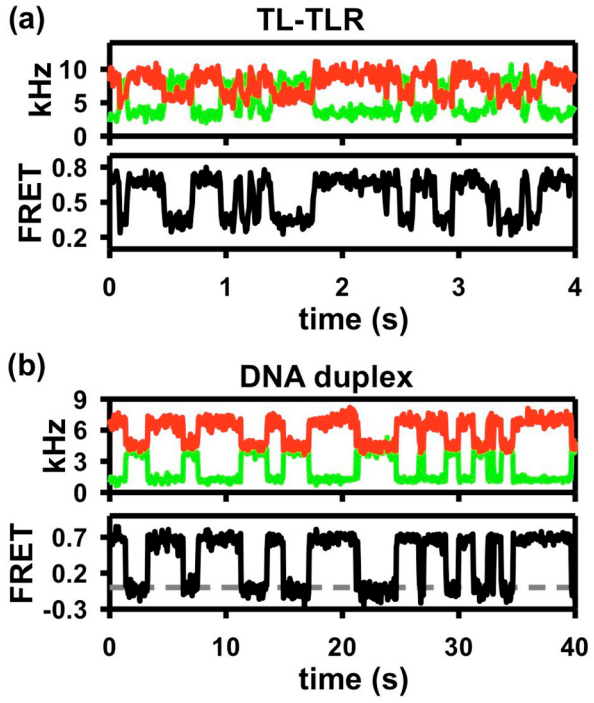

Figure 4. Representative donor (green) and acceptor (red) fluorescence and FRET trajectories for (a) the TL-TLR and (b) the DNA duplex. Analysis of the clear two-state folding behavior in the FRET trajectories (black) permits determination of the folding (k_{fold}) and unfolding (k_{unfold}) rate constants for each of the nucleic acid constructs.

$$E_{FRET} = \left(1 - \frac{\alpha_A Q_A I_D}{\alpha_D Q_D I_A}\right) \Big/ \left(1 + \frac{Q_A I_D}{Q_D I_A}\right) \quad (1)$$

Dwell times are determined from the FRET trajectories using a previously described thresholding routine.[38,41] Rate constants are extracted from cumulative distribution plots of dwell times[45−47] by performing single-exponential decay least-squares fits with weights dictated by Poissonian statistics. Temperature control of the sample is accomplished using commercially available stage and objective heaters, as described elsewhere.[40]

3. RESULTS

The two nucleic acid model constructs have been chosen for a variety of reasons. First of all, they represent the two major types of structural transitions in nucleic acids: secondary (2°) and tertiary (3°). Canonical Watson−Crick interactions within a double helix are one of the defining characteristics of nucleic acid 2° structure formation. Conversely, the GAAA tetraloop-tetraloop receptor interaction (TL-TLR) contains both non-canonical hydrogen bonding and base stacking between a loop and an internal bulge. These are among some of the distinguishing features of 3° interactions, which frequently orient and stabilize the global architecture and three- dimensional conformation of large structured nucleic acids. Furthermore, the two model constructs have been previously studied using single-molecule techniques,[34,36−42] with the results of these experiments, providing a well-characterized baseline for the folding/unfolding kinetics in the absence of osmolytes. Lastly, both the secondary and the tertiary interactions are capable of forming in the absence of Mg^{2+}. This allows K_{eq} for the conformational transitions to be "tuned" via [KCl], while also limiting the number of cosolutes in solution, which reduces the potential for complex cooperative effects observed in more complex solutions.[39]

3.1. Folding in the Absence of Osmolytes. Time-trajectories from individual surface-immobilized TL-TLR constructs demonstrate two-state folding kinetics (Figure 4a) with well-defined high and low FRET states (e.g., docked ⇔ undocked). The 8bp DNA duplex exists in a bimolecular equilibrium (e.g., dissociated ⇔ associated) with a concentration-dependent rate constant for duplex association. To facilitate rate constant determination, experiments are performed at a fixed concentration (200 nM) of the freely diffusing Cy5-labeled strand 3.[34] The surface-immobilized trajectories for the 8bp duplex also exhibit two-state kinetic behavior (Figure 4b).

The well-separated FRET states for each of the constructs make it easy to determine dwell times using a previously described thresholding routine.[39,41] The experimentally measured dwell times are analyzed via a cumulative distribution function[45−47] to determine rate constants for each construct, which establishes a point-of-comparison for experiments conducted using solutions containing high concentrations of osmolytes. For ease of discussion, the forward rate constant for both systems (i.e., duplex association and tetraloop docking) will be referred to as the folding rate constant (k_{fold}), whereas the reverse process will be referred to as the unfolding rate constant (k_{unfold}). To further facilitate kinetic and thermodynamic comparisons, KCl concentrations are adjusted so as to achieve a ratio of rate constants ($K_{eq} = k_{fold}/k_{unfold}$) that is near unity in the absence of osmolyte (see Experimental Methods).

3.2. Osmolyte-Dependent Folding Kinetics. The experimental results from single-molecule titrations with respect to TMAO and urea for both the TL-TLR (▲) and 8 bp DNA duplex (●) are presented in Figure 5, which clearly demonstrate the kinetic origin of osmolyte-influenced nucleic acid folding. Addition of TMAO increases k_{fold} and decreases k_{unfold} (Figure 5a) for each nucleic acid construct. Together, these kinetic effects contribute to an increase in K_{eq} and therefore more favorable folding, as one would expect for this stabilizing osmolyte. Qualitatively opposite trends are obtained as a function of urea, whereby elevated concentrations decrease k_{fold} and increase k_{unfold} (Figure 5b) for both the 8 bp DNA duplex and the TL-TLR, resulting in the expected decrease in K_{eq}.

However, the details associated with the above trends are notably different (Table S1 of the Supporting Information). For example, one can clearly see that (i) the impact of TMAO on k_{fold} for the TL-TLR is considerably stronger than for the 8 bp DNA duplex (Figure 5a, red ▲ vs ●), whereas (ii) urea increases k_{unfold} for the 8 bp DNA duplex much more effectively than for the TL-TLR (Figure 5b, green ▲ vs ●). These osmolyte-dependent kinetic rate constants are used to calculate equilibrium constants, which can be interpreted more quantitatively using the *m*-value analysis discussed below.

3.3. Osmolyte-Dependent Folding Free Energies (*m*-Value Analysis). With knowledge of both rate constants, the free-energy change (ΔG°_{fold}) can be readily calculated from the equilibrium constant ($K_{eq} = k_{fold}/k_{unfold}$) using the Gibbs equation ($\Delta G^\circ = -RT \ln[K_{eq}]$). As empirically observed for several nucleic acids[23,48,49] and proteins,[50,51] this folding free-energy change appears to be approximately linearly dependent on osmolyte concentration (Figure 6). This slope ($\partial\Delta G^\circ/\partial[\text{osmolyte}]$) is often characterized by the *m*-value, which serves as a measure of the folding transition's sensitivity to the presence of an osmolyte.[23] From the *m*-values in Figure 6, it is apparent that (i) TMAO is much more effective at stabilizing the TL-TLR

DOI: 10.1021/jp512491n
J. Phys. Chem. B 2015, 119, 3687−3696

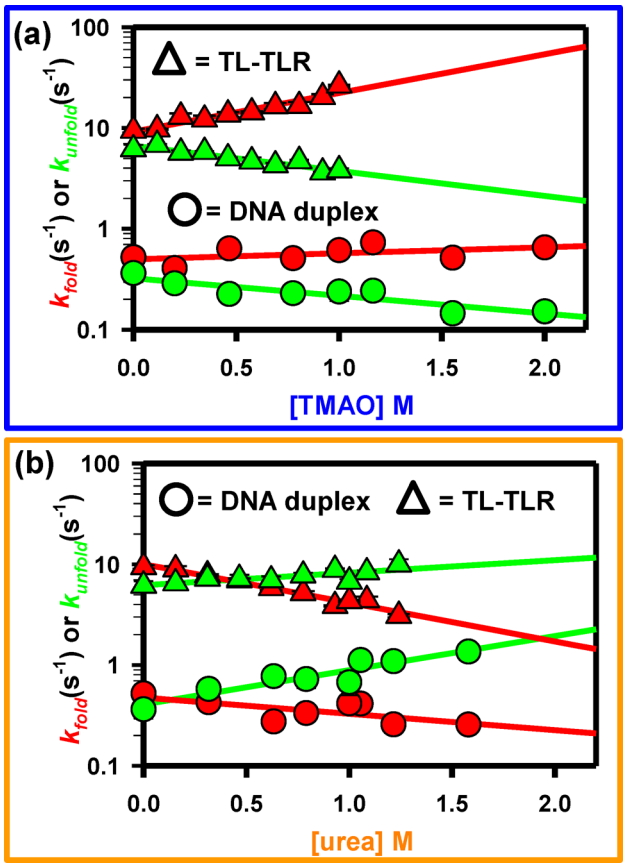

Figure 5. Kinetic origin of osmolyte-influenced nucleic acid folding for both the GAAA tetraloop—receptor (▲) and DNA duplex (●) constructs. For both constructs, the stabilizing osmolyte TMAO (blue box, top) increases k_{fold} (red symbols) and decreases k_{unfold} (green symbols), whereas the destabilizing osmolyte, urea (orange box, bottom), decreases k_{fold} (red symbols) and increases k_{unfold} (green symbols). See Table S1 of the Supporting Information for a summary of fit parameters.

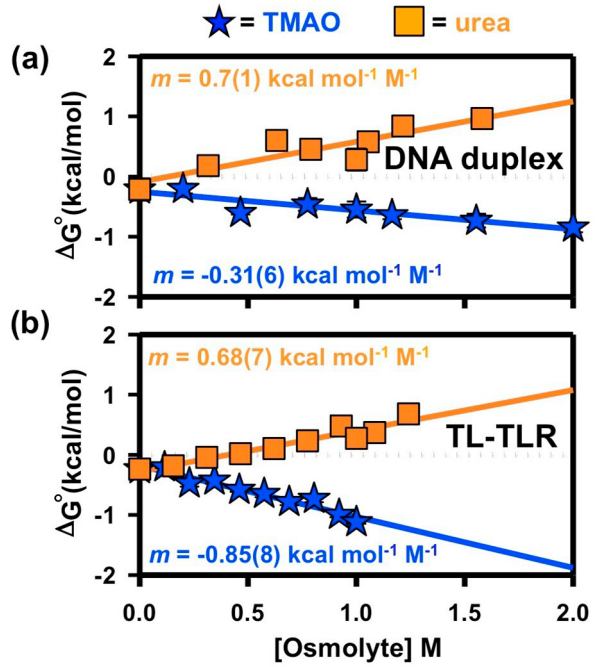

Figure 6. Osmolyte-dependent folding free-energy change for (a) the DNA duplex and (b) the TL-TLR constructs. For both constructs, addition of TMAO (blue ★) always stabilizes the folding transitions, whereas addition of urea (orange ■) destabilizes the folding transitions, as indicated by m-value analysis slope of ΔG° vs osmolyte concentration.

(m = −0.85(8) kcal/mol) than the 8 bp DNA duplex (m = −0.31(6) kcal/mol) and (ii) urea destabilizes both model constructs by nearly identical amounts (m = 0.7(1) kcal/mol and −0.68(7) kcal/mol). The equilibrium observations derived from our single-molecule kinetics experiments are in good agreement with previous ensemble equilibrium studies, which reveal that urea effectively destabilizes both 2° and 3° interactions, whereas TMAO primarily stabilizes the formation of 3° structure.

3.4. Osmolyte-Dependent Thermodynamics for the 8 bp DNA Duplex. To more rigorously explore the kinetic origins of osmolyte-influenced nucleic acid folding, temperature-dependent experiments have been performed, allowing folding free energies to be deconstructed into their enthalpic and entropic components.[37,42] Briefly, a plot of $\ln[K_{eq}]$ vs $1/T$ provides information on ΔH° and ΔS° in accordance with standard van't Hoff analyses. Similarly, the dependence of $\ln[k]$ vs $1/T$ provides information about the enthalpic and entropic components of the free-energy barrier ($\Delta H^{\ddagger}$ and $\Delta S^{\ddagger}$) in what is known as an Eyring analysis.[52,53] For example, in the linear plot of $\ln[K_{eq}]$ vs $1/T$ in Figure 7, the slope and intercept correspond to $-\Delta H^{\circ}/R$ and $\Delta S^{\circ}/R$, respectively, where R is the ideal gas constant (≈ 1.987 cal mol^{-1} K^{-1}). It is particularly noteworthy that neither osmolyte substantially changes the slope and therefore ΔH° associated with formation of the 8 bp DNA duplex (Figure 7a). This observation indicates that the thermodynamic origin of TMAO- and urea-influenced 2° structure formation is predominately entropic. Furthermore, the corresponding Eyring analyses (Figure S1b of the Supporting Information) demonstrate that there is a much larger osmolyte-induced change in $\Delta S^{\ddagger}_{unfold}$ than $\Delta S^{\ddagger}_{fold}$, which implies that these entropic considerations are largely related to the unfolding process.

Explicitly stated, TMAO stabilizes the 8 bp DNA duplex by making the unfolding barrier less entropically rewarding, whereas urea destabilizes this conformational transition by making the unfolding barrier more entropically rewarding. The thermodynamics results for the 8 bp DNA duplex prove to be in excellent agreement with the corresponding kinetic data (Figure 5, ●), confirming that the impact of both osmolytes is most prominent in the unfolding rate constant (k_{unfold}).

3.5. Osmolyte-Dependent Thermodynamics for the TL-TLR. As was the case for urea-inhibited folding of the 8 bp DNA duplex, the presence of 1 M urea has a minuscule effect on the slope and thus $\partial\Delta H^{\circ}/\partial[\text{osmolyte}] \approx 0$ for the TL-TLR interaction (Figure 7b). Once again, this indicates that entropy is the dominant thermodynamic component responsible for urea-induced destabilization. However, in contrast with the 8bp DNA duplex construct, a majority of the change in ΔS° is related to the folding process (see Figure S2 of the Supporting Information), which is well-supported by the corresponding kinetics analyses and demonstrate that destabilization occurs primarily via a reduction of k_{fold} (Figure 5b, ▲). Altogether, the kinetic and thermodynamic results confirm that urea destabilizes this 3° interaction by increasing the entropic cost associated with the folding transition state free-energy barrier.

It is worth mentioning that at a concentration of 1 M, TMAO appears to change both the ΔH° (slope) and the ΔS° (intercept) associated with the TL-TLR interaction (Figure 7b), which is

DOI: 10.1021/jp512491n
J. Phys. Chem. B 2015, 119, 3687−3696

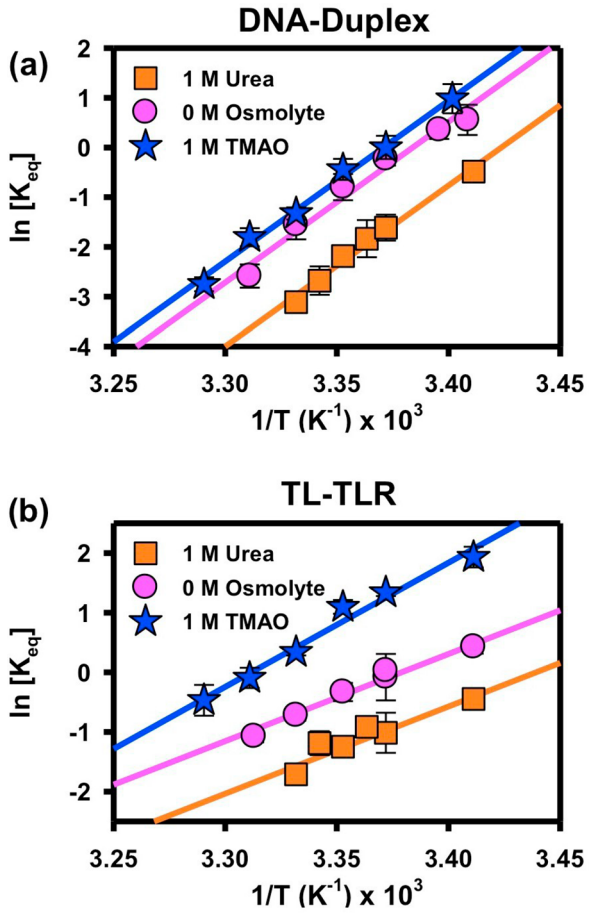

Figure 7. van't Hoff plots for the osmolyte- influenced folding of both (a) the DNA duplex and (b) the TL-TLR interaction. Solid lines in (a) correspond to a global fit with a common slope, as discussed in the text, to reduce parameter correlation between the three data sets: 1 M TMAO (blue ★), 0 M osmolyte (pink ●), and 1 M urea (orange ■). The solid lines for the TL-TLR interaction (b) are also the result of a global fit of the 0 M osmolyte and 1 M urea data sets in order to reduce parameter correlation, while the solid line for 1 M TMAO represents an individual fit of the single data set. See Table I for values of the fitted parameters.

also recapitulated in the Eyring analyses (Figure S2a of the Supporting Information). This is particularly notable because TMAO does not appear to affect the $\Delta H°$ for the 8bp DNA duplex, as evidenced by the highly parallel plots in Figure 7a. The presence of both enthalpic and entropic components in TMAO-facilitated formation of the TL-TLR reveals that this osmolyte has fundamentally distinct interactions with 2° and 3° nucleic acid constructs. This notion is rationalized in terms of differential changes in the phosphate solvent accessible surface area (SASA), as discussed below.

4. DISCUSSION

Ensemble thermal denaturation experiments have demonstrated that the *m*-value, which is a measure of the sensitivity of $\Delta G°$ to osmolyte concentration, is correlated with differences in solvent accessible surface area (SASA) between the folded and unfolded structures of nucleic acids. Specifically, the *m*-values for TMAO and urea are primarily mediated by changes in phosphate and nucleobase SASA, respectively. Vapor pressure osmometry (VPO) experiments have revealed that TMAO primarily forms unfavorable interactions with the phosphate backbone, and to a lesser extent, the nucleobases of a nucleic acid.[15] This is different from the favorable interaction between urea and the nucleobase of an oligonucleotide.[16] Accordingly, TMAO will preferentially destabilize conformations with more phosphate SASA, whereas urea will stabilize structures with greater base SASA (Figure 1). Unsurprisingly, unfolded conformations commonly have more phosphate and base SASA than their folded counterparts, meaning that TMAO stabilizes nucleic acid folding transitions, whereas urea destabilizes them (Figure 1).

4.1. TMAO–Dependent Folding Free Energies. The folding/unfolding rate constants (Figure 5) are used to calculate equilibrium constants ($K_{eq} = k_{fold}/k_{unfold}$) that are used to determine the osmolyte-dependence of the free-energy change for folding (i.e., *m*-value). These results clearly indicate that TMAO is better able to stabilize tertiary (e.g., TL-TLR), rather than secondary (e.g., DNA duplex), structural transitions (Figure 6). Previous calculations based on structural models of duplex nucleic acids predict very little change in phosphate SASA upon formation of a double helix,[4] which would render TMAO an ineffective stabilizing osmolyte. However, VPO experiments[15] indicate that there are some weak but still energetically unfavorable, interactions between TMAO and nucleobases that would result in a net stabilization of the duplex based on the change in nucleobase SASA. Conversely, the substantial change in phosphate SASA (≈ 67 Å^2) for the TL- TLR receptor interaction[15] clearly explains why TMAO is significantly more effective at stabilizing this structural transition. Together, these TMAO-dependent folding results bolster the notion that, when changes in phosphate SASA are substantial, TMAO can quite effectively stabilize conformational transitions. However, when these changes are negligible, TMAO can still facilitate folding, although less efficiently, based on differences in the nucleobase SASA.

Alternatively, recent computational investigations have proposed a different mechanism for TMAO-based stabilization of nucleic acids that is dependent on the protonation of this osmolyte.[29] Specifically, the local environment of the RNA gives rise to an increase in the pK_a of TMAO leading to partial protonation. These positively charged osmolytes could then favorably interact with the negative electrostatic potential of the RNA as monovalent cations. Although, it is not apparent how such a partial protonation mechanism would vary substantially depending on the type of nucleic acid conformational transition. Nevertheless, a multi-disciplinary approach that brings together rich information from ensemble, single-molecule, and molecular dynamics investigations will be critical for the development of a complete theoretical framework describing osmolyte nucleic acid interactions.

4.2. Urea-Dependent Folding Free Energies. It is worth noting that the *m*-values for urea-induced destabilization of the TL-TLR and 8 bp DNA duplex interactions are surprisingly similar (Figure 6), which suggests nearly identical changes in nucleobase SASA for the two folding transitions. Previous ensemble experiments on similar constructs under comparable conditions yield qualitatively consistent *m*-values for urea-inhibited folding.[16,23] By way of example, a 10 bp RNA duplex at 0.5 M NaCl has an *m*-value = 0.74(4) kcal mol^{-1} molar^{-1}[54] and a bimolecular, dimeric TL-TLR construct has an extrapolated *m*-value ≈ 0.64 kcal mol^{-1}molal^{-1} at 85 mM KCl.[16] Both of these ensemble observations are within experimental uncertainty of the single-molecule *m*-values reported herein. Such excellent agreement between *m*-values measured using single-molecule techniques and ensemble UV-melting experiments further

DOI: 10.1021/jp512491n
J. Phys. Chem. B 2015, 119, 3687–3696

Table 1. Results from the Individual and Global van't Hoff Analyses of the Osmolyte-Influenced Folding of Nucleic Acids[a]

thermodynamic parameters from individual and global van't Hoff analyses						
interaction	duplex	duplex	duplex	TL-TLR	TL-TLR	TL-TLR
[osmolyte] M	$\Delta H°$ kcal mol^{-1}	$\Delta H°$ kcal mol^{-1}	$\Delta S°$ cal mol^{-1} K^{-1}	$\Delta H°$ kcal mol^{-1}	$\Delta H°$ kcal mol^{-1}	$\Delta S°$ cal mol^{-1} K^{-1}
1 M TMAO	−65(6)[b]	−65(3)[c]	−218.1(2)[d]	−41(3)[b]	n/a	−137(11)[b]
no osmolyte	−63(6)[b]	−65(3)[c]	−218.8(2)[d]	−31(3)[b]	−29(2)[c]	−97.07(8)[d]
1 M urea	−65(5)[b]	−65(3)[c]	−221.5(2)[d]	−28(4)[b]	−29(2)[c]	−99.82(8)[d]

[a]Additional information on the fitting methods for the van't Hoff plots can be found in text. See Figure 7 for full plots of the corresponding experimental data. [b]Enthalpy or entropy values from individual linear fits to the van't Hoff plots of $\ln[K_{eq}]$ vs $1/T$. [c]Enthalpy values from a global fit of the appropriate data sets with a common enthalpy change (slope). [d]Entropy values from a global fit of the appropriate data sets with a common enthalpy change (slope).

support the notion that urea is a strongly destabilizing osmolyte for both 2° and 3° folding transitions, resulting primarily from favorable interactions with the nucleobase SASA of nucleic acids. Despite similar *m*-values, which are related to the folding equilibria (i.e., k_{fold}/k_{unfold}), the pronounced structural differences between the TL-TLR and the 8bp DNA duplex results in distinct urea-dependencies for each constructs folding/unfolding rate constants.

4.3. Kinetic Origins of Osmolyte-Influenced Nucleic Acid Folding. To our knowledge, this work details the first demonstration of the kinetic origins associated with osmolyte-influenced nucleic acid folding. Specifically, the observed increase in stability of folded nucleic acid structures at elevated concentrations of TMAO is the result of an increase in k_{fold} and a decrease in k_{unfold} (Figure 5a). Alternatively, the decrease in stability associated with urea addition occurs due to a combination of a decrease in k_{fold} and an increase in k_{unfold} (Figure 5b). The notion of preferential interactions with (i) nucleobase, (ii) sugar, and (iii) phosphate SASA of nucleic acids can also be applied to osmolyte-dependence of the rate constants. Such an analysis provides qualitative information about changes in SASA that result from forming the transition state. For example, the observation that k_{fold} for the 8 bp DNA duplex construct is only slightly increased by the presence of TMAO (Figure 5a, ●) indicates that there is very little reduction in phosphate SASA upon reaching the transition state. Conversely, k_{fold} for TL-TLR construct is much more strongly accelerated by TMAO (Figure 5a, ▲), which implies a considerable reduction in phosphate SASA taking place prior to crossing the folding free-energy barrier.

Similarly, the urea-dependence of the rate constants can be used to make inferences about where nucleobase SASA burial occurs along the reaction coordinate for the two conformational transitions. Because k_{fold} for the TL-TLR interaction is much more sensitive to urea than k_{unfold} (Figure 5b), it is evident that most of the change in nucleobase SASA occurs prior to formation of the transition state. This is in contrast with previous smFRET studies of urea-induced denaturation of other RNA folding motifs (i.e., the human telomerase RNA pseudoknot,[55] the adenine riboswitch,[32] and the P4−P6 domain of the *Tetrahymena* ribozyme[46]) where addition of urea predominantly affects the unfolding rate constant. It is interesting to note that our TL-TLR construct reflects only one of two tertiary interactions in the much larger and more structurally complex P4−P6 domain of the *Tetrahymena* ribozyme. Thus, differences in the urea-dependent kinetics for these two constructs can arise from very different folding reaction coordinates, specifically regarding changes in the nucleobase SASA.

Accordingly, our results demonstrate not only the kinetic origins of osmolyte-influenced nucleic acid folding (Figure 5) but also that osmolytes (specifically TMAO and urea) can serve as useful experimental probes for structural information regarding changes in SASA across the entire folding landscape. For example, the large amount of nucleobase and phosphate SASA buried upon formation of the transition state for the TL-TLR interaction provides evidence for a transition state where the GAAA tetraloop and the receptor are proximal to one another. Such a structural depiction is in excellent agreement with independent single-molecule experiments, which also propose a compact transition state for this interaction.[42]

4.4. Osmolyte-Dependent Entropy Changes for the 8bp DNA Duplex. Temperature-dependent smFRET experiments have been performed to obtain insights into the thermodynamic origins (i.e., enthalpic vs entropic contributions) of osmolyte-influenced nucleic acid folding. For example, neither 1 M TMAO nor 1 M urea significantly alters the folding enthalpy, as supported by the highly parallel (vertically offset) van't Hoff plots for the 8 bp DNA duplex (Figure 7a). This observation both demonstrates that (i) $\Delta H°$ is insensitive to the presence of osmolytes (Table 1) and (ii) the predominant source of the osmolyte-dependent $\Delta G°$ (*m*-value) must result from entropic considerations. Previous calorimetric experiments that examined the effect of destabilizing osmolytes (e.g., urea) on DNA melting have similarly concluded that entropic terms dominate, giving rise to the observed decrease in duplex stability.[17] Additionally, computational simulations of an RNA hairpin (e.g., 2° structure) in the presence of TMAO suggest that, if the interaction between the two is unfavorable, then this osmolyte will act like a small-molecule crowding agent that entropically stabilizes the folded conformation.[28] With these findings in mind, it is important to note that our single-molecule thermodynamic results provide further support for the notion that the osmolyte-induced changes in $\Delta G°$ for 2° structure formation result from entropic terms (Figure 7a). This would suggest that free-energy changes, resulting from expulsion of TMAO (or urea) from surfaces buried in the process of forming 2° structure, are dominated by entropic rewards (or costs), respectively. Such an entropic description is analogous with the so-called depletion interaction observed in TMAO-facilitated protein folding, whereby TMAO is depleted from regions near the peptide backbone resulting in the stabilization of compact conformations with less solvent accessible surface area. Indeed, one possible interpretation of the similarly entropic nature of both TMAO-facilitated biomolecular folding and molecular crowding[43] could be that this osmolyte acts as a nanocrowding solute,[26] at least for proteins and nucleic acid secondary structure formation. However, such characterization must clearly offer only a piece of the full story, as an entropically dominated description of the thermodynamics does not appear to be equally valid for nucleic acids tertiary structure formation (see Sec. 4.6).

DOI: 10.1021/jp512491n
J. Phys. Chem. B 2015, 119, 3687−3696

To more quantitatively explore the osmolyte-dependence of the entropy change associated with duplex formation and to reduce parameter correlation between ΔH° and ΔS° for the individual data set in isolation,[56] the three data sets (i.e., 1 M TMAO, 0 M osmolyte, and 1 M urea) have been globally refit with common slopes and independent intercepts (Table 1). The resulting values of ΔS° are able to explain ≈ 80% of the osmolyte-dependence for ΔG°(295 K), which is entirely consistent with the notion of an entropic origin for urea-inhibited or TMAO-facilitated duplex formation. An Eyring analysis of the temperature-dependent rate constants (Figure S1 of the Supporting Information) unites the kinetic and thermodynamic origins of these processes by demonstrating that most of the change in ΔS° is associated with the unfolding free energy barrier (i.e., $-T\Delta S^{\ddagger}_{unfold}$). Stated more generally, TMAO stabilizes nucleic acid 2° structure formation by decreasing k_{unfold} via a decrease in the entropic reward associated with the unfolding barrier, whereas urea destabilizes 2° structure formation by increasing k_{unfold}, which results from an unfolding barrier that is more entropically rewarding.

4.5. Urea-Dependent Entropy Changes for the TL-TLR. Temperature-dependent van't Hoff analysis of the TL-TLR data makes it evident that addition of 1 M urea primarily results in an entropic destabilization of the 3° interaction (Figure 7b). The results from the global analysis reveal that the urea-induced changes to ΔS° account for ≈ 74% of the *m*-value at 295 K (Table 1). Furthermore, most of the change in ΔS° is associated with the folding barrier (Figure S2 of the Supporting Information). This observation is internally consistent with the kinetic origin of urea-inhibited folding of the TL-TLR, which reveals that k_{fold} is more prominently affected than k_{unfold} (Figure 5b, ▲). Together, the kinetic and thermodynamic results suggest that urea destabilizes the TL-TLR by predominantly decreasing k_{fold} via an increase in the entropic cost associated with the folding barrier. Alternatively stated, urea is expelled from the buried nucleobase SASA as the RNA surmounts the folding barrier, which is largely an entropically unfavorable process.

Single-molecule urea-induced denaturation studies of an RNA pseudoknot[55] also demonstrate a largely entropic destabilization; however, they result from a strong increase in k_{unfold} rather than a decrease in k_{fold}, as observed for the TL-TLR. This observation suggests that individual tertiary interactions will exhibit kinetics whose dependencies on urea are quantitatively different, but that destabilization by urea is likely always of entropic origin. It is also worth noting that because of the canonical base pairing in both the RNA pseudoknot and the 8 bp DNA duplex, it is unsurprising that urea predominately affects k_{unfold} for these two folding transitions (RNA pseudoknot and DNA duplex), as they are very similar with respect to changes in nucleobase SASA.

4.6. Alternative Mechanism for TMAO–Dependent Entropy Changes in the TL-TLR. As a parting comment, we return to the issue of phosphate SASA and its relationship to TMAO-facilitated stabilization mechanisms for both secondary and tertiary structures. Although the kinetic origin of TMAO-facilitated formation of the TL-TLR is qualitatively similar to that of the 8bp DNA duplex (i.e., k_{fold} increases and k_{unfold} decreases), the thermodynamics of this process are in fact noticeably different. Specifically, 1 M TMAO significantly decreases ΔH°, and folding becomes more exothermic for the TL-TLR construct, as evidenced by the steeper slopes in Figure 7b, which is not observed for the 8bp DNA duplex (Figure 7a). More quantitatively, the least-squares results reveal that both ΔH° and ΔS° decrease with the addition of 1 M TMAO (Table 1), which clearly identifies a thermodynamically distinct mechanism for TMAO-induced stabilization of the TL-TLR that is different from the entirely entropic mechanism associated with the 8bp DNA duplex.

One clear difference between tertiary and secondary folding events is the amount of phosphate SASA burial incurred. For folding transitions with substantial decrease in phosphate SASA (e.g., 3° structure formation), the expulsion of TMAO from these surfaces must be both exothermic and entropically costly. For the TL-TLR interaction, most of this change in phosphate SASA occurs prior to formation of the transition state (Figure 5a and Figure S2 of the Supporting Information).

Addition of 1 M TMAO results in a net increase in k_{fold} at 295 K because of the TMAO-induced decrease in $\Delta H^{\ddagger}_{fold}$ is greater than the decrease in $T\Delta S^{\ddagger}_{fold}$ (Figure S2 of the Supporting Information). The different thermodynamic origins for TMAO-stabilized folding of the 8 bp DNA duplex and TL-TLR constructs highlight two potential pathways by which TMAO can interact with and influence nucleic acid folding: (i) strong, unfavorable TMAO–phosphate interactions driven by entropic and enthalpic terms, resulting in efficient stabilization of nucleic acid conformational transitions with large changes in phosphate SASA and (ii) weak, unfavorable, predominately entropic interactions between TMAO and the nucleobase that stabilize nucleic acid folding transitions with negligible changes in phosphate SASA.

Finally, although these single-molecule experiments explicitly demonstrate the kinetic and thermodynamic effects of TMAO and urea on two model constructs, it remains unknown how general these observations may be, both with respect to different osmolytes (e.g., glycine betaine, proline, sucrose, etc.) as well as different nucleic acid secondary versus tertiary structural motifs (e.g., pseudoknots, G-quadruplexes, kissing loops, etc.). Indeed, further exploration of the role of osmolytes in promoting nucleic acid folding transitions, guided by single-molecule experiments focused on both the kinetic and thermodynamic origins, will likely prove crucial in developing a more complete theoretical framework for nucleic acid conformational dynamics in cosolute-rich cellular environments.

5. CONCLUSIONS

Single-molecule fluorescence techniques have been used to observe the effect of stabilizing (TMAO) and destabilizing (urea) osmolytes on the folding/unfolding rate constants for both an 8 bp DNA duplex and the GAAA tetraloop—tetraloop receptor (TL-TLR) motif. The results demonstrate that, regardless of the type of the nucleic acid conformational transition (i.e., secondary or tertiary), TMAO always stabilizes nucleic acid structure formation by increasing the folding rate constant and decreasing the unfolding rate constant, although this effect is much more pronounced for tertiary structure formation. Conversely, urea always destabilizes nucleic acid structure formation by decreasing the folding rate constant and increasing the unfolding rate constant. However, the magnitude of these osmolyte-induced changes to the folding/unfolding rate constants are dependent on the amount and type (e.g., nucleobase or phosphate) of solvent accessible surface area (SASA) that is buried for each of the conformational transitions.

Complementary temperature-dependent single-molecule kinetic studies of the 8bp DNA duplex reveal that osmolyte-induced stabilization or destabilization results almost entirely from changes to the entropic component of the unfolding free-energy barrier, regardless of the osmolyte. For the TL–TLR

DOI: 10.1021/jp512491n
J. Phys. Chem. B 2015, 119, 3687–3696

interaction, these studies demonstrate that urea destabilizes the structural equilibrium by increasing the entropic penalty associated with the folding barrier. However, the thermodynamic origin of TMAO-facilitated formation of this structural motif is quite distinct, whereby a favorable increase in exothermicity out competes an increase in entropic cost associated with the folding free-energy barrier. These two effects highlight significant thermodynamic differences between TMAO-facilitated formation of secondary and tertiary structure.

The experimental observations from this work elucidate both the kinetic and thermodynamic origins of osmolyte-influenced nucleic acid conformational transitions. These findings will likely provide valuable information for development and refinement of theoretical descriptions of osmolyte-nucleic acid interactions. Of special interest, our detailed characterization demonstrates how osmolytes can be used as biochemical tools to map out changes in SASA during a particular folding transition. Lastly, this work begins to unveil how small neutral organic molecules that are highly soluble in cells and biological tissues may potentially influence the structural dynamics of functional nucleic acids. This suggests that future single-molecule efforts should be profitably directed at studying the effects of other biologically relevant osmolytes, such as those that function in the renal medulla of the kidney[57] (e.g., glycine betaine, sorbitol, and taurine).

■ ASSOCIATED CONTENT

Supporting Information

Table S1 summarizes the fitted parameters from Figure 5, and Figures S1 and S2 depict the results of the Eyring analyses for the 8bp DNA duplex and TL-TLR construct, respectively. This material is available free of charge via the Internet at http://pubs.acs.org.

■ AUTHOR INFORMATION

Corresponding Author

*E-mail: djn@colorado.edu. Tel: (303) 492-8857. Fax: (303) 493-5235.

Notes

The authors declare no competing financial interest.

■ ACKNOWLEDGMENTS

Support for this work has been provided by the National Science Foundation (Grants CHE1266416 and PHYS1125844), the National Institute of Standards and Technology, and the W. M. Keck Foundation initiative in RNA sciences at the University of Colorado, Boulder. The National Institutes of Health Molecular Biophysics Training Program (T32 GM-065103) and the National Research Council have provided partial support for E.D.H. and N.F.D., respectively.

■ REFERENCES

(1) Draper, D. E. A Guide to Ions and RNA Structure. *RNA* **2004**, *10* (3), 335−343.
(2) Klein, D. J.; Moore, P. B.; Steitz, T. A. The Contribution of Metal Ions to the Structural Stability of the Large Ribosomal Subunit. *RNA* **2004**, *10* (9), 1366−1379.
(3) Kurz, M. Compatible Solute Influence on Nucleic Acids: Many Questions but Few Answers. *Saline Syst.* **2008**, *4* (6), 1−14.
(4) Lambert, D.; Draper, D. E. Effects of Osmolytes on RNA Secondary and Tertiary Structure Stabilities and RNA-Mg^{2+} Interactions. *J. Mol. Biol.* **2007**, *370* (5), 993−1005.
(5) Blose, J. M.; Pabit, S. A.; Meisburger, S. P.; Li, L.; Jones, C. D.; Pollack, L. Effects of a Protecting Osmolyte on the Ion Atmosphere Surrounding DNA Duplexes. *Biochemistry* **2011**, *50* (40), 8540−8547.
(6) Yancey, P. H.; Clark, M. E.; Hand, S. C.; Bowlus, R. D.; Somero, G. N. Living With Water Stress: Evolution of Osmolyte Systems. *Science* **1982**, *217* (4566), 1214−1222.
(7) Record, M. T., Jr.; Courtenay, E. S.; Cayley, D. S.; Guttman, H. J. Responses of E. coli to Osmotic Stress: Large Changes in Amounts of Cytoplasmic Solutes and Water. *Trends Biochem. Sci.* **1998**, *23* (4), 143−148.
(8) Hu, C.; Rösgen, J.; Pettitt, B. M. Osmolyte Influence on Protein Stability: Perspectives of Theory and Experiment. In *Modeling Solvent Environments*; Wiley-VCH: Weinheim, Germany, 2010; pp 77−92.
(9) Yancey, P. H.; Somero, G. N. Counteraction of Urea Destabilization of Protein Structure by Methylamine Osmoregulatory Compounds of Elasmobranch Fishes. *Biochem. J.* **1979**, *183* (2), 317−323.
(10) Record, M. T., Jr.; Courtenay, E. S.; Cayley, S.; Guttman, H. J. Biophysical Compensation Mechanisms Buffering E. coli Protein-Nucleic Acid Interactions Against Changing Environments. *Trends Biochem. Sci.* **1998**, *23* (5), 190−194.
(11) Liu, Y.; Bolen, D. W. The Peptide Backbone Plays a Dominant Role in Protein Stabilization by Naturally Occurring Osmolytes. *Biochemistry* **1995**, *34* (39), 12884−12891.
(12) Timasheff, S. N. Control of Protein Stability and Reactions by Weakly Interacting Cosolvents: The Simplicity of the Complicated. *Adv. Protein Chem.* **1998**, *51*, 355−432.
(13) Courtenay, E. S.; Capp, M. W.; Saecker, R. M.; Record, M. T., Jr. Thermodynamic Analysis of Interactions Between Denaturants and Protein Surface Exposed on Unfolding: Interpretation of Urea and Guanidinium Chloride m-Values and Their Correlation With Changes in Accessible Surface Area (ASA) Using Preferential Interaction Coefficients and the Local-Bulk Domain Model. *Proteins* **2000**, *S4*, 72−85.
(14) Courtenay, E. S.; Capp, M. W.; Anderson, C. F.; Record, M. T., Jr. Vapor Pressure Osmometry Studies of Osmolyte-Protein Interactions: Implications for the Action of Osmoprotectants in vivo and for the Interpretation of "Osmotic Stress" Experiments in vitro. *Biochemistry* **2000**, *39* (15), 4455−4471.
(15) Lambert, D.; Leipply, D.; Draper, D. E. The Osmolyte TMAO Stabilizes Native RNA Tertiary Structures in the Absence of Mg^{2+}: Evidence for a Large Barrier to Folding from Phosphate Dehydration. *J. Mol. Biol.* **2010**, *404* (1), 138−157.
(16) Lambert, D.; Draper, D. E. Denaturation of RNA Secondary and Tertiary Structure by Urea: Simple Unfolded State Models and Free Energy Parameters Account for Measured m-Values. *Biochemistry* **2012**, *51* (44), 9014−9026.
(17) Spink, C. H.; Garbett, N.; Chaires, J. B. Enthalpies of DNA Melting in the Presence of Osmolytes. *Biophys. Chem.* **2007**, *126* (1−3), 176−185.
(18) Hong, J.; Capp, M. W.; Anderson, C. F.; Saecker, R. M.; Felitsky, D. J.; Anderson, M. W.; Record, M. T., Jr. Preferential Interactions of Glycine Betaine and of Urea With DNA: Implications for DNA Hydration and forEffects of These Solutes on DNA Stability. *Biochemistry* **2004**, *43* (46), 14744−14758.
(19) Felitsky, D. J.; Cannon, J. G.; Capp, M. W.; Hong, J.; Van Wynsberghe, A. W.; Anderson, C. F.; Record, M. T., Jr. The Exclusion of Glycine Betaine From Anionic Biopolymer Surface: Why Glycine Betaine is an Effective Osmoprotectant but Also a Compatible Solute. *Biochemistry* **2004**, *43* (46), 14732−14743.
(20) Bennion, B. J.; Daggett, V. The Molecular Basis for the Chemical Denaturation of Proteins by Urea. *Proc. Natl. Acad. Sci. U.S.A.* **2003**, *100* (9), 5142−5147.
(21) Greene, R. F., Jr.; Pace, C. N. Urea and Guanidine Hydrochloride Denaturation of Ribonuclease, Lysozyme, Alpha-Chymotrypsin, and Beta-Lactoglobulin. *J. Biol. Chem.* **1974**, *249* (17), 5388−5393.
(22) Tanford, C. Isothermal Unfolding of Globular Proteins in Aqueous Urea Solutions. *J. Am. Chem. Soc.* **1964**, *86* (10), 2050−2059.

DOI: 10.1021/jp512491n
J. Phys. Chem. B 2015, 119, 3687−3696

(23) Shelton, V. M.; Sosnick, T. R.; Pan, T. Applicability of Urea in the Thermodynamic Analysis of Secondary and Tertiary RNA Folding. *Biochemistry* **1999**, *38* (51), 16831−16839.
(24) Canchi, D. R.; Garcia, A. E. Cosolvent Effects on Protein Stability. *Annu. Rev. Phys. Chem.* **2013**, *64*, 273−293.
(25) Schwinefus, J. J.; Kuprian, M. J.; Lamppa, J. W.; Merker, W. E.; Dorn, K. N.; Muth, G. W. Human Telomerase RNA Pseudoknot and Hairpin Thermal Stability With Glycine Betaine and Urea: Preferential Interactions with RNA Secondary and Tertiary Structures. *Biochemistry* **2007**, *46* (31), 9068−9079.
(26) Cho, S. S.; Reddy, G.; Straub, J. E.; Thirumalai, D. Entropic Stabilization of Proteins by TMAO. *J. Phys. Chem. B* **2011**, *115* (45), 13401−13407.
(27) Wang, A. J.; Bolen, D. W. A Naturally Occurring Protective System in Urea-Rich Cells: Mechanism of Osmolyte Protection of Proteins against Urea Denaturation. *Biochemistry* **1997**, *36* (30), 9101−9108.
(28) Pincus, D. L.; Hyeon, C.; Thirumalai, D. Effects of Trimethylamine N-oxide (TMAO) and Crowding Agents on the Stability of RNA Hairpins. *J. Am. Chem. Soc.* **2008**, *130* (23), 7364−7372.
(29) Denning, E. J.; Thirumalai, D.; MacKerell, A. D., Jr. Protonation of Trimethylamine N-oxide (TMAO) is Required for Stabilization of RNA Tertiary Structure. *Biophys. Chem.* **2013**, *184*, 8−16.
(30) Priyakumar, U. D.; Hyeon, C.; Thirumalai, D.; MacKerell, A. D. Urea Destabilizes RNA by Forming Stacking Interactions and Multiple Hydrogen Bonds with Nucleic Acid Bases. *J. Am. Chem. Soc.* **2009**, *131* (49), 17759−17761.
(31) Yoon, J.; Thirumalai, D.; Hyeon, C. Urea-Induced Denaturation of preQ1-Riboswitch. *J. Am. Chem. Soc.* **2013**, *135* (32), 12112−12121.
(32) Dalgarno, P. A.; Bordello, J.; Morris, R.; St-Pierre, P.; Dube, A.; Samuel, I. D.; Lafontaine, D. A.; Penedo, J. C. Single-Molecule Chemical Denaturation of Riboswitches. *Nucleic Acids Res.* **2013**, *41* (7), 4253−4265.
(33) Tinoco, I.; Gonzalez, R. L. Biological Mechanisms, One Molecule at a Time. *Genes Dev.* **2011**, *25* (12), 1205−1231.
(34) Dupuis, N. F.; Holmstrom, E. D.; Nesbitt, D. J. Single-Molecule Kinetics Reveal Cation- Promoted DNA Duplex Formation Through Ordering of Single-Stranded Helices. *Biophys. J.* **2013**, *105*, 756−766.
(35) Fiore, J. L.; Nesbitt, D. J. An RNA Folding Motif: GNRA Tetraloop-Receptor Interactions. *Q. Rev. Biophys.* **2013**, *46* (3), 223−64.
(36) Fiore, J. L.; Holmstrom, E. D.; Fiegland, L. R.; Hodak, J. H.; Nesbitt, D. J. The Role of Counterion Valence and Size in GAAA Tetraloop-Receptor Docking/Undocking Kinetics. *J. Mol. Biol.* **2012**, *423*, 198−216.
(37) Fiore, J. L.; Holmstrom, E. D.; Nesbitt, D. J. Entropic Origin of Mg^{2+}-Facilitated RNA Folding. *Proc. Natl. Acad. Sci. U.S.A.* **2012**, *109* (8), 2902−2907.
(38) Downey, C. D.; Fiore, J. L.; Stoddard, C. D.; Hodak, J. H.; Nesbitt, D. J.; Pardi, A. Metal Ion Dependence, Thermodynamics, and Kinetics for Intramolecular Docking of a GAAA Tetraloop and Receptor Connected by a Flexible Linker. *Biochemistry* **2006**, *45* (11), 3664−3673.
(39) Fiore, J. L.; Hodak, J. H.; Piestert, O.; Downey, C. D.; Nesbitt, D. J. Monovalent and Divalent Promoted GAAA-Tetraloop−Receptor Tertiary Interactions from Freely Diffusing Single-Molecule Studies. *Biophys. J.* **2008**, *95* (8), 3892−3905.
(40) Fiore, J. L.; Kraemer, B.; Koberling, F.; Erdmann, R.; Nesbitt, D. J. Enthalpy-Driven RNA Folding: Single-Molecule Thermodynamics of Tetraloop−Receptor Tertiary Interaction. *Biochemistry* **2009**, *48*, 2550−2558.
(41) Hodak, J. H.; Downey, C. D.; Fiore, J. L.; Pardi, A.; Nesbitt, D. J. Docking Kinetics and Equilibrium of a GAAA Tetraloop-Receptor Motif Probed by Single-Molecule FRET. *Proc. Natl. Acad. Sci. U.S.A.* **2005**, *102* (30), 10505−10510.
(42) Holmstrom, E. D.; Fiore, J. L.; Nesbitt, D. J. Thermodynamic Origins of Monovalent Facilitated RNA Folding. *Biochemistry* **2012**, *51* (18), 3732−3743.
(43) Dupuis, N. F.; Holmstrom, E. D.; Nesbitt, D. J. Molecular Crowding Effects on Single Molecule RNA Folding/Unfolding Thermodynamics and Kinetics. *Proc. Natl. Acad. Sci. U.S.A.* **2014**, *111* (23), 8464−8469.
(44) Aitken, C. E.; Marshall, R. A.; Puglisi, J. D. An Oxygen Scavenging System for Improvement of Dye Stability in Single-Molecule Fluorescence Experiments. *Biophys. J.* **2008**, *94* (5), 1826−1835.
(45) Blanco, M.; Walter, N. G. Analysis of Complex Single-Molecule FRET Time Trajectories. *Methods Enzymol.* **2010**, *472*, 153−178.
(46) Bartley, L. E.; Zhuang, X. W.; Das, R.; Chu, S.; Herschlag, D. Exploration of the Transition State for Tertiary Structure Formation Between an RNA Helix and a Large Structured RNA. *J. Mol. Biol.* **2003**, *328* (5), 1011−1026.
(47) Zhou, Y. J.; Zhuang, X. W. Robust Reconstruction of the Rate Constant Distribution Using the Phase Function Method. *Biophys. J.* **2006**, *91* (11), 4045−4053.
(48) Sclavi, B.; Woodson, S.; Sullivan, M.; Chance, M. R.; Brenowitz, M. Time-Resolved Synchrotron X-Ray "Footprinting", a New Approach to the Study of Nucleic Acid Structure and Function: Application to Protein-DNA Interactions and RNA Folding. *J. Mol. Biol.* **1997**, *266* (1), 144−159.
(49) Pan, J.; Thirumalai, D.; Woodson, S. A. Folding of RNA Involves Parallel Pathways. *J. Mol. Biol.* **1997**, *273* (1), 7−13.
(50) Pace, C. N. The Stability of Globular Proteins. *Crit. Rev. Biochem.* **1975**, *3* (1), 1−43.
(51) Myers, J. K.; Pace, C. N.; Scholtz, J. M. Denaturant m-Values and Heat Capacity Changes: Relation to Changes in Accessible Surface Areas of Protein Unfolding. *Protein Sci.* **1995**, *4* (10), 2138−2148.
(52) Abdelaal, Y. A. I.; Hammock, B. D. Use of Transition-State Theory in the Development of Bioactive Molecules. *ACS Symp. Ser.* **1985**, *276*, 135−160.
(53) Laidler, K. J.; King, M. C. The Development of Transition-State Theory. *J. Phys. Chem.* **1983**, *87* (15), 2657−2664.
(54) Shelton, V. M.; Sosnick, T. R.; Pan, T. Applicability of Urea in the Thermodynamic Analysis of Secondary and Tertiary RNA Folding. *Biochemistry* **1999**, *38* (51), 16831−19839.
(55) Holmstrom, E. D.; Nesbitt, D. J. Single-Molecule Fluorescence Resonance Energy Transfer Studies of the Human Telomerase RNA Pseudoknot: Temperature-/Urea-Dependent Folding Kinetics and Thermodynamics. *J. Phys. Chem. B* **2014**, *118* (14), 3853−3863.
(56) Cornish-Bowden, A. Enthalpy-Entropy Compensation: A Phantom Phenomenon. *J. Biosci. (New Delhi, India)* **2002**, *27* (2), 121−126.
(57) Burg, M. B. Coordinate Regulation of Organic Osmolytes in Renal Cells. *Kidney Int.* **1996**, *49* (6), 1684−1685.

DOI: 10.1021/jp512491n
J. Phys. Chem. B 2015, 119, 3687−3696